

Correlation length in cuprate superconductors deduced from impurity-induced magnetization

S. Ouazi¹, J. Bobroff¹, H. Alloul¹, W.A. MacFarlane¹
¹LPS, UMR 8502, 91405 Orsay Cedex, France

We report a new multinuclei based nuclear magnetic resonance method which allows us to image the staggered polarization induced by nonmagnetic Li impurities in underdoped ($O_{6.6}$) and slightly overdoped (O_7) $YBa_2Cu_3O_{6+y}$ above T_C . The spatial extension of the polarization ξ_{imp} approximately follows a Curie law, increasing up to six lattice constants at 80K at $O_{6.6}$ in the pseudogap regime. Near optimal doping, the staggered magnetization has the same shape, with ξ_{imp} reduced by a factor 2. ξ_{imp} is argued to reveal the intrinsic magnetic correlation length of the pure system. It is found to display a smooth evolution through the pseudogap regime.

I- INTRODUCTION

In high T_C cuprates, strong antiferromagnetic (AF) correlations reminiscent of the AF ordered phase were often argued to explain the anomalous normal state properties of the CuO_2 planes and to lead to the d-wave pairing in the superconducting state [1]. Nuclear magnetic resonance (NMR) and neutron scattering experiments both showed the existence of such correlations and their decrease with increasing doping. However, no agreement has been reached about quantitative determinations of the AF correlation length ξ values and about a possible incommensurability. In underdoped $YBa_2Cu_3O_{6+y}$, some neutron experiments detect a magnetic response peak with a temperature (T) independent q width, which corresponds to $\xi \approx 2.5$ (in lattice units) [2]. But this response could be dominated by a macroscopic inhomogeneity in the large single crystals used or according to other experiments an incommensurability, so that ξ could be underestimated. In contrast, the analysis of Pines *et al.* (noted hereafter MMP) of the Cu NMR relaxation times T_1 and T_2 suggests a Curie-Weiss behavior for ξ which might reach values as large as 7 at 100K [3]. But, various reexaminations of the MMP analysis lead to substantial uncertainties in their ξ values, so that at $O_{6.6}$, a model-free determination of ξ versus T is still lacking. Near optimal doping, the magnetic response peak measured by neutrons broadens a lot and its intensity is reduced indicating smaller magnetic correlations. This makes the experimental data difficult to analyse quantitatively.

We propose to use nonmagnetic impurities to determine this length scale ξ in cuprates. Nonmagnetic substitutions on the magnetic sites of low dimensionnal AF correlated systems are known to lead to the appearance of

an AF staggered magnetization. This has been observed by NMR in cuprates [4] [5] [6], spin chains [7], and spin ladders [8]. In the case of an AF $S = 1$ spin chain, the induced polarization could be imaged site by site [7]. Its extension was found to be identical to the correlation length of the pure system. In the same spirit, we propose a detailed quantitative study of the staggered magnetization induced by nonmagnetic Li and Zn substituted at the Cu sites of CuO_2 planes in $YBa_2Cu_3O_{6+y}$. Previous studies proved that the staggered polarization has a non-Fermi liquid T dependence, confirming the correlated nature of the planes [5]. However, no quantitative determination of the extent or shape of this polarization could be achieved. It is not yet clear whether the decay of the spin polarization can be described by a single length scale. One can indeed wonder whether charge and spin degrees of freedom can result in different responses. Here, we measure the modifications induced by nonmagnetic impurities on the NMR spectra of all the available nuclei, ^{17}O , ^{89}Y and the 7Li impurity itself. Combining all these informations we determine, for the first time, the shape of the impurity induced polarization on a significantly large lengthscale and deduce that a single lengthscale ξ_{imp} can be used.

This "multinuclei" analysis allows us to deduce the spatial variation of the polarization with temperature and doping. We demonstrate that ξ_{imp} increases with decreasing temperature in the pseudogap phase. This polarization persists, but is reduced in O_7 , out of the pseudogap phase, together with the Kondo-type T variation of its magnitude evidenced in [9]. Comparison with the MMP analysis suggests that ξ_{imp} is, as in spin chains, a direct measure of the correlation length ξ of the pure system.

The paper is organized as follows: Sec. II is devoted to the description of samples and of the NMR experimental conditions. In Sec. III we describe the principle of our multinuclei method. In Sec. IV, we present the experimental results. The next two sections are concerned with the description and analysis of the experimental results. We detail in Sec. V the steps for determining the induced magnetization and present our results for the induced magnetism at $O_{6.6}$ and O_7 . A comparison with neutron experiments in Zn substituted O_7 is discussed in Sec. VI. We compare also quantitatively our findings with the neutron scattering and nuclear spin relaxation measurements in the pure YBCO compound.

II- EXPERIMENTAL DETAILS

NMR measurements presented hereafter were done on $YBa_2(Cu_{1-x_N}Li_{x_N})_3O_{6+y}$ compounds with $x_N = 0, 0.01$

and 0.02. According to measurements done in [9] on the same samples, a quantity $x_{plane} = 0.85 \times x_N$ of Li is found to substitute the Cu site of the planes. For all the samples, the ^{17}O enrichment procedure was carried out as in [5]. The samples were fully reoxidized at 300°C leading to the slightly overdoped composition $y = 1$ (noted hereafter as O_7). Deoxidation of part of each batch allowed to produce the underdoped samples $y = 0.6$ ($\text{O}_{6.6}$) under thermogravimetric control. The powders were finally aligned in Stycast epoxy in a high magnetic field so that their c axis could then be chosen to lie parallel to the NMR static field. Our samples present a misorientation of less than 10° of the c axis which introduces a second order quadrupolar broadening of the Cu spectra but has negligible effect on the ^{89}Y spectrum and on the central transition of the ^{17}O NMR. We performed ^{17}O , ^{89}Y , ^7Li measurements at O_7 and $\text{O}_{6.6}$ (some of the ^{89}Y and ^7Li NMR data at $\text{O}_{6.6}$ were already published in [9]). Spectra were obtained using Fourier Transform of the echoes obtained with a standard $(\pi/2) - \tau - \pi$ sequence under typical fields H_{ext} of 7 Tesla. We also performed ^{63}Cu NMR measurements in the underdoped compound at 300K and 100K in a 5Tesla applied field.

III- MULTINUCLEI METHOD

The key point of our multinuclei method is that each nuclear species is coupled differently to the electronic spin density on the Cu sites, i.e., they have different hyperfine form factors [10]. This was already judiciously used in the pure system to distinguish between uniform and antiferromagnetic spin fluctuations through T_1 measurements [3]. We proceed in the same spirit for the impurity problem. We assume that an impurity positioned at the origin induces a polarization $\langle S^z(\vec{r}, T) \rangle$ noted S_n^m on the Cu site at $\vec{r} = (m, n)$ in lattice units from the impurity. The ^{17}O nucleus is predominantly coupled to the spin density of its two copper neighbors and has an NMR resonance shifted by :

$$^{17}K(m, n) = ^{17}\alpha(S_n^m + S_n^{m+1})$$

where $^{17}\alpha = ^{17}A_{hf}g/H_{ext}$, $^{17}A_{hf}$ is the hyperfine coupling between ^{17}O and one Cu site in the c direction of the measurements and g is the Landé factor. The other nuclei follow in the same manner:

$$^{89}K(m, n) = ^{89}\alpha(S_n^m + S_n^{m+1} + S_{n+1}^m + S_{n+1}^{m+1}),$$

$$^{63}K(m, n) = ^{63}\alpha\left(\frac{A}{B}S_n^m + S_n^{m+1} + S_n^{m-1} + S_{n+1}^m + S_{n-1}^m\right),$$

$$^7K(0, 0) = ^7\alpha * 4 * S_0^1$$

where A and B are respectively the Cu on-site and nearest neighbor supertransferred hyperfine couplings [11]. Due to its specific position, the ^7Li shift probes only the polarization of the $r = 1$ Cu near neighbors (noted nn). For the other nuclei, the different geometrical factors act like filters. To illustrate this effect, in Fig.1 we plot the

magnitude of these shifts $|K(m, 0)|$ along the $(1, 0)$ direction and on checkerboards for an exponentially decaying polarization. For an alternated polarization, the ^{17}O

shift $^{17}K(m, n)$ measures a quantity which roughly corresponds to the 1st derivative of the polarization envelope. Similarly, the ^{89}Y shift $^{89}K(m, n)$ rather represents the curvature of the polarization envelope. The more complex filtering operated by the shift measurement of ^{63}Cu combines both a direct contribution of the spin polarization and of its derivatives. From these couplings, it can be intuitively understood that the various nuclei will not be sensitive to the same range of the polarization. This can be seen in Fig. 1, where, for a given polarization, we represent the local shifts using the proper filter for each nucleus. Furthermore, for each nuclear species, the existence of various sources of NMR line broadening in the pure materials limits the experimental sensitivity and defines a cut-off on the distance which can be probed. This leads us to conclude that ^{89}Y primarily probes the nearfield ($r < 3$) of the polarization whereas ^{17}O is sensitive to $r \lesssim 8$. The comparison between NMR spectra of these different nuclei should then allow to recover an information on a large range of distances. We note that ^{63}Cu NMR in principle probes the full range and might thus appear the ideal probe to determine the whole polarization. Unfortunately the experimental conditions are not sufficient to exploit the ^{63}Cu NMR spectra for a quantitative analysis, as will be detailed hereafter.

IV- EXPERIMENTAL RESULTS

Our measurements show indeed qualitatively different features for these various nuclei. This confirms that these nuclei do not probe the same spatial ranges of the Cu spin polarization. In underdoped $\text{O}_{6.6}$ samples, two well separated satellites appear in the ^{89}Y NMR spectra as shown in Fig. 2. They correspond to the first and second nn to the Li as anticipated from Fig. 1. The ^{17}O NMR spectra do not show such satellites, but are symmetrically broadened by the impurities as shown in the inset of Fig. 3. This broadening has a faster T -variation than that of the ^{89}Y satellites shift which follows a Curie-like variation. The ^7Li NMR shift also follows a $1/T$ Curie law in the T -range measured here [9]. As for the ^{63}Cu NMR, the large second order quadrupole effects makes it extremely sensitive in pure samples on the preparation conditions and on the quality of the alignment of the powder. So it is hard to compare accurately the spectra of pure and substituted samples. We have however measured between 300K and 100K an absolute increase of the linewidth of $23000 \pm 4000\text{ppm}$ for 2% Li. Although these numbers will be useful for comparison with the data on the other nuclei, we considered that a systematic study of the Cu NMR in our specific experimental conditions would not be useful. This will be discussed further in Sec. V B 1.

In slightly overdoped O_7 , the impurity effects on the NMR spectra are not only strongly reduced but also dis-

play a qualitative change in their T dependences. Discrete NMR satellite resonances are no more detectable in the ^{89}Y spectra which only exhibit a slight broadening which varies roughly as $1/T$ (see the inset of Fig. 2). The ^{17}O width also increases as $1/T$ (see Fig. 3) while the ^7Li shift follows a $1/(T+135)$ Curie-Weiss behavior. The behaviors of the ^{89}Y and the ^{17}O spectra both at $\text{O}_{6.6}$ and O_7 are qualitatively very similar to those observed in Zn-substituted compounds. Their magnitude only differ by at most 20% from that observed on Li substituted samples for the same in-plane impurity concentration. Therefore, the observations done for Li impurities can be considered as universal signatures of nonmagnetic impurity effects in cuprates.

V- DETERMINATION OF THE INDUCED MAGNETIZATION

We now apply the multinuclei analysis to these findings in order to reconstruct the induced polarization. We performed extensive numerical simulations in order to fit the data, constrain the shape of the corresponding polarization, and deduce its amplitude and the T dependence of its extension. Our methodology is detailed in Sec. V A, in the regime where the measurements show the largest impurity-induced changes, i.e., in the $\text{O}_{6.6}$ compound at the lowest temperatures. We demonstrate that a single length scale and shape actually describes the spatial dependence of the polarization. In Sec. V B this methodology has been systematically applied versus temperature. It allows us to present our main results, i.e., the spatial characterization of the induced magnetism from an underdoped compound $\text{O}_{6.6}$ up to a slightly overdoped compound O_7 .

A. Methodology

To get quantitative information from these experimental observations, let us write the local AF polarization as such:

$$\langle S^z(\vec{r}, T) \rangle = -S_0^1 (-1)^{m+n} f_T(r) \quad (1)$$

where $f_T(\vec{r})$ is the envelope of the staggered polarization at a temperature T which is normalized to $f_T(\vec{r}) = 1$ for $\|\vec{r}\| = 1$.

The hyperfine couplings of the pure compounds are known for all nuclei [11] and can be retained for nuclear sites which are not nearest neighbors of the impurities. However, the hyperfine coupling $^{89}\text{A}_{hf}^1$ between the ^{63}Cu and ^{89}Y nearest neighbors of the same Li impurity is expected to be modified. The ^7Li hyperfine coupling $^7\text{A}_{hf}$ is not known accurately as well. The analysis done below will allow us to constrain their values.

We have performed numerical simulations of the ^{89}Y and ^{17}O spectra for various choices of amplitude S_0^1 and shape $f_T(\vec{r})$ on a checkerboard of $150 * 150$ cells, with a concentration x_{plane} of randomly distributed impurities.

In Sec. V A 1, we demonstrate that the experimental features of the ^{17}O and ^{89}Y NMR can only be accounted for by a continuous exponentially shaped polarization and hence by only one length scale. In Sec. V A 2 the ^{17}O spectrum shape further allows us to determine S_0^1 , and therefore $^{89}\text{A}_{hf}^1$ and $^7\text{A}_{hf}$.

1. Shape and continuity of the spin polarization

At a given temperature S_0^1 is initially unknown and the ^{89}Y first satellite NMR shift is not useful here to analyse the polarization shape. At $\text{O}_{6.6}$, the final amplitude S_0^1 and shape $f_T(\vec{r})$ must account for (i) the presence of two ^{89}Y satellites on the spectrum, (ii) the shift of the second ^{89}Y satellite and (iii) the Lorentzian like shape of the ^{17}O line.

We shall illustrate on the 80K data the analysis done at various temperatures. First we use the experimental features of the ^{89}Y spectrum to constrain the polarization envelope at short distances from the impurity. The assumption of a given amplitude S_0^1 at 80K leads to a unique choice for $f_T(\vec{r})$ for which only two ^{89}Y satellites distinct from the central line exist. This can be clearly seen in Fig. 4. For a given amplitude S_0^1 , different curvatures A , B and C lead to ^{89}Y spectra with qualitatively different spectral structures. Only one of them (B) presents two satellites and fit the second satellite shift. The decay C is too smooth to produce two satellites distinct from the central line. The sharper curvature A leads to a third satellite not observed experimentally. Moreover, this polarization shape cannot account quantitatively for the second satellite position. On the contrary, the exponentially decaying B accounts well for both the presence of two satellites and the value of the shift of the second satellite. Hence ^{89}Y data allows to constrain $f_T(\vec{r})$ up to the fourth Cu sites ($r \leq \sqrt{5}$) for a given choice of S_0^1 . Anyhow, different solutions for different S_0^1 are still compatible with the experiments. This is exemplified in Fig. 4 where both B and D polarizations represented in the inset of Fig. 4 lead to ^{89}Y spectra with only two satellites and the second one at the proper position.

In order to constrain the shape $f_T(\vec{r})$ at further distances, we use now the ^{17}O spectra. Let us consider as an example the short range polarization envelope represented by the curve B in Fig. 4. For $r \geq \sqrt{5}$, we free the shape in order to account for the experimental spectrum. Figure 5 represents simulated ^{17}O spectra and their corresponding polarizations. The only satisfying fit is obtained for an exponential curvature which prolongates the short distance decay B . A polarization with two different length scales results in a more complex spectral shape. This is exemplified by the simulated spectra in Fig. 5. The experimental smooth lorentzian spectrum can only be explained by a continuous exponentially shaped envelope. On the spectra corresponding to discontinuous polarizations, a satellite or shoulders appear on the ^{17}O spectra. This allows then to exclude

the scenario in which a large induced moment appears on a short length scale and yields a longer range spin polarization.

2. Amplitude

To determine now the polarization amplitude S_0^1 , we attempt fits of the experimental ^{17}O spectrum with the various possible short range polarizations which correspond to distinct S_0^1 such as D and E (see Fig. 6). We let the polarization shape free for $r \geq \sqrt{5}$. The Lorentzian ^{17}O experimental spectrum can be fit at best by the represented curvatures. The shape required for $r \geq \sqrt{5}$ is again found exponential and continuous with the short range curvature. But all these cases do not fit the ^{17}O spectrum equally well. Case D results in an ^{17}O spectrum with shoulders and case E can not explain quantitatively the broadening. Eventhough D , B and E all account for ^{89}Y spectra only B accounts as well for the ^{17}O shape and width at the same temperature.

Thus ^{17}O NMR allows to select the proper amplitude S_0^1 , and therefore yields a value for the Li hyperfine coupling ${}^7A_{hf}$ through $S_0^1(T = 80) = {}^7K(T = 80K) H_{ext}/4{}^7A_{hf}g$. Taking into account the experimental accuracy, we found that ${}^7A_{hf}$ ranges from 0.85 to 1.05kOe. This result is consistent with our previous upper experimental estimation ${}^7A_{hf} < 2.5kOe$ [9], done from the comparison with the measured susceptibility. The value S_0^1 also allows us to determine the ^{89}Y first satellite shift and the first nn ^{89}Y hyperfine field ${}^{89}A_{hf}^1 = 0.8 \times {}^{89}A_{hf}$, which only slightly differs from that of the bulk.

For increasing T , the ^{89}Y experimental spectrum always presents two satellites and the ^{17}O lineshape remains Lorentzian. Hence the polarization envelope shape has to be exponential at all temperatures, and a single length scale ξ_{imp} is necessary to describe it. In the following, we choose the Bessel functional form $f_T(r) = K_0(r/\xi_{imp})/K_0(1/\xi_{imp})$, which approximates an exponential $exp(-2r/\xi_{imp})$ for the experimental range of values of r/ξ_{imp} explored. This mathematical notation is used here rather than the exponential one as it is exactly that which appears in the MMP analysis of the relaxation data. The fact that the same analytical definition is taken for ξ_{imp} and ξ in the two approaches will allow us to compare them quantitatively.

B. Results

As shown above the experimental data constrains a Bessel-type polarization shape at each temperature. Its extension ξ_{imp} is then directly determined by the ^{17}O impurity-induced broadening.

1. Induced magnetism in underdoped $O_{6.6}$

The corresponding findings for $\xi_{imp}(T)$ are presented in Fig. 7, the upper (lower) bounds of the error bars being associated with the higher (lower) limit for ${}^7A_{hf}$. Our central results consists then in the restricted range of a couple of values for the amplitude S_0^1 and the extension $\xi_{imp}(T)$ of the staggered polarization. From the obtained values of $\xi_{imp}(T)$, we could compute the ^{89}Y satellites positions over the full range of temperatures. Those are found to agree reasonably well with the experimental ones as can be seen in Fig. 2. This confirms *a posteriori* the validity of our analysis and of the value obtained for ${}^{89}A_{hf}^1$.

To check further the coherence of the analysis we computed the corresponding ^{63}Cu spectra and compared them to the experimental ones. At 100K, our simulations lead to a ^{63}Cu broadening between 22000ppm and 25000ppm. This value is very similar to our measured broadening. But a quantitative comparison between the experimental Cu spectra and the simulated ones requires to pay further attention to some experimental complications. Recent Nuclear Quadrupole Resonance experiments evidenced that nuclei up to at least the fourth nn of the impurities are undetectable due to relaxation effects or to an impurity contribution to the electric field gradient [12]. As such effects should then occur as well in our NMR measurements, we measured the x_N dependence of the ^{63}Cu NMR intensity. Assuming that a nucleus either fully participates to the NMR line, or is merely wiped out, we estimated a cutoff radius of about four unit cells (slightly smaller than that of [12]). We then computed the expected impurity-induced broadening of the Cu spectrum when this wipe out is taken into account. This broadening is reduced to a value between 16000 and 18000ppm, slightly smaller than the experimental value of 23000ppm. Other ^{63}Cu measurements have been done on a single crystal sample with a similar Zn concentration but with slightly larger hole doping [6]. They show an impurity-induced broadening of 12600ppm at 100K, almost 2 times smaller than ours. For this data taken in different experimental conditions (external field, sample doping, and dopant), comparisons beyond order of magnitude agreement cannot be performed.

To conclude this comparison with ^{63}Cu NMR data an overall agreement is obtained, but the experimental complications mentioned above prevents getting any further information from the NMR spectra in our experimental conditions.

2. Induced magnetism in slightly overdoped O_7

As the hyperfine couplings are usually found independent of doping in cuprates, the value of ${}^7A_{hf}$ determined from the $O_{6.6}$ analysis can be kept, so the data for ${}^7K(T)$ directly yield the values of S_0^1 . Hereagain, the Lorentzian shape of the ^{17}O NMR line constrains an exponential shape for the polarization envelope, and the impurity-induced broadening directly allowed us to deduce $\xi_{imp}(T)$, which is plotted in Fig. 7. The corre-

sponding ^{89}Y simulated satellite positions are plotted in the inset of Fig. 2. They appear much less shifted from the main line than at $\text{O}_{6.6}$. This is expected, as the Li shift indicates that the polarization on the first nn Cu is much smaller than in $\text{O}_{6.6}$. A convolution with the typical lineshape of the pure sample allows us to confirm that such satellites cannot be resolved in agreement with the data, but contribute to the broadening of the ^{89}Y line which fits the experimental one.

3. Comparison with the macroscopic susceptibility data

Finally we compute the impurity contribution to the macroscopic susceptibility χ_{imp} which is given by the sum of $\langle S^z(\vec{r}) \rangle$ on all Cu sites of the checkerboard. At $\text{O}_{6.6}$, the computed χ_{imp} follows a Curie-Weiss law in $p_{eff}^2/(T + \Theta)$ with $\Theta < 100\text{K}$ and an effective magnetic moment $p_{eff} = 1.5(3)\mu_B$ per impurity. This behavior agrees within our uncertainties with the Curie law measured in Zn-substituted high purity compounds [13]. At O_7 , the calculated χ_{imp} is also compatible with these data, as it presents a strong reduction mostly due to an increase of Θ . This confirms the robustness of our analysis. This variation of the Curie-Weiss temperature detected on the first nn has been attributed to a Kondo-type screening of the induced moment by the carriers [9]. From Eq. (1), we find here that this Kondo-type T dependence merely multiplies the whole AF response. This situation is similar to the standard Kondo effect in dilute alloys where $\langle S^z(\vec{r}, T) \rangle = \langle S_{impurity}^z(T) \rangle f(r)$ [14]. However in our case the impurity itself is not magnetic and the function $f(r)$ actually depends on T as a consequence of the variation of ξ .

VI- DISCUSSION

A. Comparison to other impurity studies

Let us compare now our findings to the existing experimental studies. Our induced magnetization model is compatible with previous NMR measurements [4] [5] [6] in YBCO with nonmagnetic Zn impurities. Inelastic neutrons scattering (INS) measurements performed on $\text{O}_7 + \text{Zn}$ have evidenced that Zn substitutions enhance low energy AF fluctuations [15]. The q width of the inelastic peak at the AF wave vector Q_{AF} reveals a length scale ξ_n of 1.3 cell units at 150K and 1.6 cell units just above T_c . This length scale obtained either with a Lorentzian or Gaussian fit of the peak is very similar to our result (Fig. 8). The neutron peak results from the superposition of the impurity induced AF fluctuations on the contribution of the pure system. It is then difficult to attribute a simple significance to ξ_n . On the contrary, in our analysis, we deal only with the impurity-induced magnetism. The quantitative agreement between these

results is therefore quite surprising but might indicate that these length scales are not that different, at least for O_7 . On the other side, the longitudinal spin lattice relaxation T_1 of ^7Li [16] relates directly to the low frequency response probed by INS. The present determination of $^7A_{hf}$ allows us to estimate the electronic fluctuation time τ of the nn induced magnetic moment. It corresponds to an energy scale $\hbar/\tau = (18.4 \pm 3.7)\text{meV}$ at 100K in O_7 (independently of Li concentration) [17] very similar to the value $15 \pm 3\text{meV}$ observed by INS in O_7 with 1.6% Zn [18]. Thus at O_7 , in presence of 1.6% Zn, the fluctuation time of the induced moments is also coherent with the energy of the impurity-induced AF fluctuations measured by INS. We however stress here that the present NMR experiments allow to separate unambiguously the impurity-induced magnetism from the pure one. Our method gives the spatial dependence of the staggered magnetization and its temperature dependence, and allowed us to probe as well the induced magnetism in the underdoped regime.

Various theoretical studies show that the AF correlations in the pure compound are responsible for the appearance of an AF polarization near a spin vacancy. Weak coupling AF spin fluctuation models lead to a polarization similar to ours within RPA [19]. Strong coupling models such as t-J or Resonating Valence Bond also anticipate the observed polarization, at least qualitatively [20]. However, contrary to the case of undoped spin chains none of these approaches have attempted to establish a relation between the extension of the induced magnetism and the correlation length in the pure compound.

Let us now compare the polarization extension ξ_{imp} near the impurities to the correlation length ξ as obtained from experimental studies on the pure compounds.

B. Comparison to the MMP analysis

Indirect information can be obtained through the analysis of T_1 and T_2 ^{63}Cu NMR measurements as done by MMP. At O_7 , the MMP analysis yields a nearly constant $\xi \simeq 2$ between 100K and 200K , represented on figure 8. Within the error bars, this value is very close to our value of ξ_{imp} . In contrast, in the underdoped regime, we find a value of ξ_{imp} at room T about 5 times smaller than that deduced by MMP for ξ , and a much larger T dependence (see figure 8). However, the MMP analysis relies on T_2 which can be strongly affected by the occurrence of the intrabilayer coupling and also by a possible incommensurability. These effects both lead to an overestimate of ξ , especially at $\text{O}_{6.6}$ [21] [22]. Hence, the only reliable estimates from the MMP analysis are those done for O_7 . At this doping, the similarity between ξ_{MMP} and our ξ_{imp} is therefore a good indication that the impurity reveals the correlation length of the pure compound. The much better experimental accuracy obtained for $\xi_{imp}(T)$ as compared to ξ_{MMP} implies that ξ nearly varies as $1/T$

at O_7 . At $O_{6.6}$, our determination of $\xi_{imp}(T)$ should then presumably also represent the T variation of ξ .

C. Comparison to INS measurements in the pure compounds

INS experiments in pure compounds in principle allow to probe ξ through the q width of the AF peak ($(1/\Delta q) \propto \xi$), when detectable. Incommensurabilities of the AF response might yield a broadening which leads then to an overestimate of Δq . Hence neutrons usually give a lower bound for ξ . Our results are compatible with previous INS results if taking into account a possible incommensurability or energy dependance of the neutrons data (see Fig. 8, in [2]). But the absence of any T variation of the AF peak seen by INS *a priori* contrasts with our observations.

First, these INS experiments probe high energy fluctuations, contrary to NMR which measures the zero-energy limit. Aeppli *et al.* in pure LSCO (almost optimally doped [23]) showed the existence of an energy dependence for Δq . When the energy is lowered, Δq is reduced at low T and enhanced at high T . This suggests that the correlation length measured at low energy could still behave similarly to our data for ξ_{imp} . A recent theoretical work [24] proposes a spin excitation function $\chi''(q, \omega)$ with a small plateau around Q_{AF} which would reconcile as well the T -independent q width of the neutrons peak in the pure system with our T -dependent ξ_{imp} .

Of course an incommensurability δ of the magnetic response, as evidenced in pure underdoped compounds by some neutrons experiments [25] might as well explain this apparent discrepancy. We considered whether such a value for δ would play a role in the analysis of our results. This should yield a large-range modulation of $f_T(r)$ which should vanish at a distance of about eight or nine unit cells. Fortunately, this effect does not affect the staggered magnetism at short distances probed by ^{89}Y and ^{17}O . We found that the changes induced in our simulated ^{17}O spectra would not be detected within experimental accuracy. So our determination of $\langle S^z(r, T) \rangle$ for $r \lesssim 8$ is therefore unaffected. In contrast ^{63}Cu nuclei probe the polarization at larger distances than ^{89}Y and ^{17}O and might be sensitive to such an incommensurability. But probing the staggered magnetization at $r > 8$ might only be ensured after securing that the observations are not affected by interactions between impurities. Determining the shape of the tail of the polarization with ^{63}Cu NMR thus requires a much better experimental resolution, i.e., high quality single crystals with $x_{plane} \ll 1\%$.

In summary, we have compared the impurity induced polarization extension $\xi_{imp}(T)$ to the correlation length $\xi(T)$ estimated in the pure compounds. We found that these quantities are similar to that obtained from the MMP analysis in the optimally doped samples. Various possible sources for a broadening of the INS AF peak in the underdoped samples have been proposed. This lets

us suggest that the spatial range $\xi_{imp}(T)$ of the induced magnetization around an impurity might be the best estimate of $\xi(T)$.

VII-CONCLUSION

In conclusion, we have used NMR to determine the shape and magnitude of the staggered polarization induced by a nonmagnetic impurity. We have found that the decay of the polarization is characterized by a single length scale, and is best fitted by an exponential. This detailed information obtained gives a new basic constraint on any microscopic model of cuprates. This experiment allows us to demonstrate that the AF correlations in the normal state of YBCO persist up to optimal doping with no qualitative abrupt change when crossing the pseudogap line. The extension ξ_{imp} of the staggered polarization is found sizeable and T dependent in both the underdoped and slightly overdoped regimes. We suggest that this quantity might be the best estimate of the actual correlation length in the pure systems, although further theoretical support for this proposal is still required.

ACKNOWLEDGEMENTS

The authors would like to thank G. Aeppli, P. Bourges, B. Keimer, P. Mendels and Y. Sidis for constructive discussions.

FIGURE 1 : Magnitude of the local shifts $|K(m, n)|$ at the ^{17}O (b), ^{89}Y (c) and ^{63}Cu (d) nuclei for $H//c$ from an impurity-induced polarization S_n^m as represented in absolute values in (a) as function of the distance to the impurity along the (1,0) direction. The checkerboards (insets) show the same quantities on the bidimensional CuO_2 layer. Black color is for the maximum intensity and each square corresponds to one nucleus. In (b), the ^{17}O neighbor sites to the impurity (hatched area) - not observed up to now - are not considered here as they only sense one Cu site, and should undergo a large shift.

FIGURE 2 : Data for the shift with respect to the main ^{89}Y line of the two satellites resonances detected at $O_{6.6}$. A reference spectrum taken at 100K is displayed. The computed satellite shifts with the parameters values given in Fig. 6 are shown as gray lines. The inset displays the equivalent figure for the O_7 case, and shows that the satellites cannot be resolved.

FIGURE 3 : Broadening of the NMR spectrum of the planar oxygens induced by Li impurities with $x_N = 2\%$ for $O_{6.6}$ (triangles) and O_7 (circles). The broadening of the line in pure compound has been subtracted. In the inset is displayed a typical Lorentzian spectrum for $O_{6.6}$ with $x_N = 2\%$ Li at 80K. The small "bump" in the low frequency tail corresponds to the resonance line of the apical site, almost completely attenuated by dynamical contrast (fast repetition time).

FIGURE 4 : Comparison of the experimental ^{89}Y spectrum at 80K in $\text{O}_{6.6}$ to simulated ones and their corresponding polarization (inset). Dotted line indicates the experimental satellite shift. Polarizations A , B and C have the same amplitude at $r = 1$ but different curvatures. They lead to the computed spectra A , B , and C . For this given amplitude, only the B exponential decay account for the experimental features. For a different $r = 1$ amplitude, the polarization D leads to simulated spectrum D which can also account for the experimental shape. On these simulated spectra, the first satellite position does not coincide with the experimental, as we use the value $^{89}A_{hf}$ of the pure compound for the hyperfine coupling between ^{89}Y and ^{63}Cu nn of the Li.

FIGURE 5 : Comparison of the experimental ^{17}O spectrum (thick gray line) at 80K in $\text{O}_{6.6}$ with $x_N = 2\%$ of Li to the simulated ones with the corresponding polarizations in insert, with same symbols. The short range polarization is fixed to the B case of Fig. 4. The shape of the polarization for $r > \sqrt{5}$ is varied to fit the experimental spectrum. A convolution of the computed spectra by a Lorentzian function corresponding to the broadening of the pure sample has been performed.

FIGURE 6 : Comparison of the experimental ^{17}O spectrum at 80K in $\text{O}_{6.6}$ with $x_N = 2\%$ of Li to simulated ones (b) with the corresponding polarizations in (a), with the same symbols. For these different amplitudes D , B and E , the best fit of the experimental spectrum is obtained with an exponential curvature. Among these three cases, only B can account both for the shape and the broadening of the spectrum.

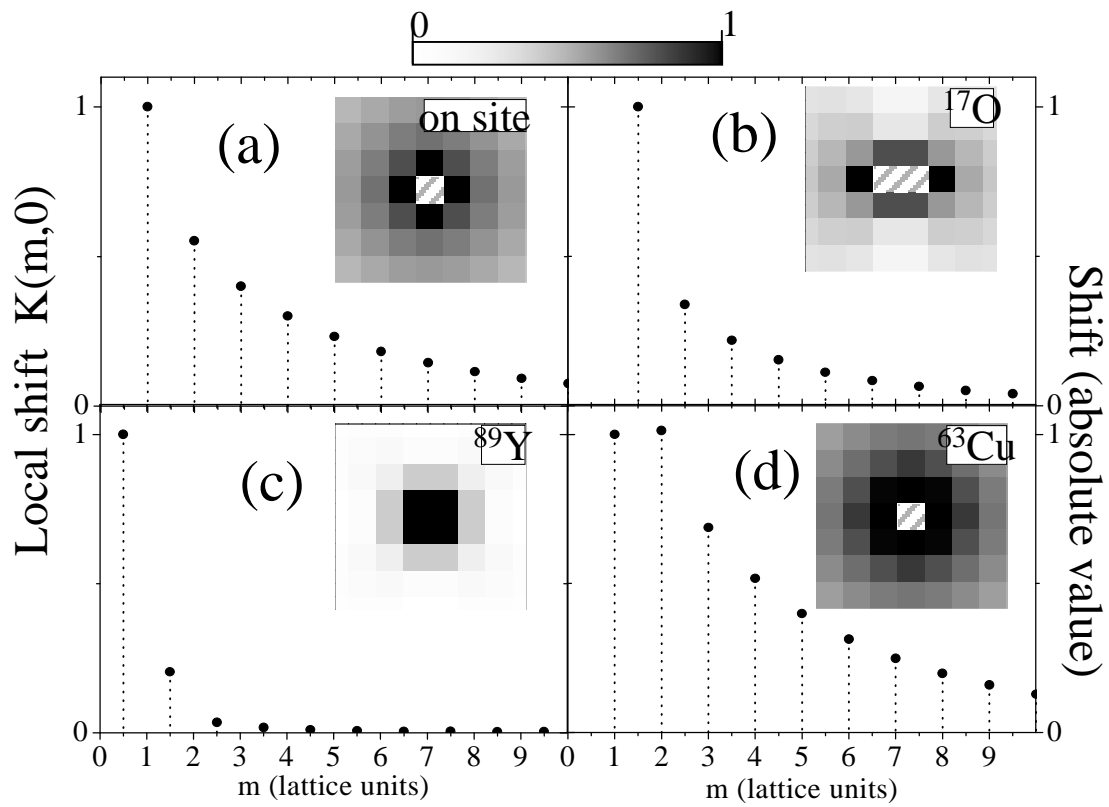
FIGURE 7 : Polarization extension ξ_{imp} (as defined in the text) as function of temperature for underdoped $\text{O}_{6.6}$ (closed circles) and slightly overdoped O_7 (open circles). The inset shows the polarization envelope at 80K for $\text{O}_{6.6}$ and O_7 .

FIGURE 8 : Comparison of our result for the polarization extension ξ_{imp} to the correlation length ξ in pure compounds extracted from INS experiments ([2]) and the MMP analysis ([3]). We plot also at O_7 the characteristic length ξ_n of the additional AF fluctuations observed in presence of Zn on the INS spectra ([15]).

[1] A.P. Kampf, Phys. Rep. **249**, 219 (1994)
[2] A.V. Balatski and P.Bourges, Phys. Rev. Lett. **82**, 5337 (1999)
[3] A.J. Millis, H. Monien, and D. Pines, Phys. Rev. B **42**, 167 (1990); V. Barzykin and D. Pines, Phys. Rev. B **52**, 13585 (1995)
[4] A.V. Mahajan, H. Alloul, G. Collin and J.F. Marucco, Phys. Rev. Lett. **72**, 3100 (1994)

[5] J. Bobroff, H. Alloul, Y. Yoshinari, A. Keren, P. Mendels, N. Blanchard, G. Collin and J.-F. Marucco, Phys. Rev. Lett. **79**, 2117 (1997)
[6] M.-H. Julien, T. Fehér, M. Horvatic, C. Berthier, O.N. Bakharev, P. Ségransan, G. Collin and J.-F. Marucco, Phys. Rev. Lett. **84**, 3422 (2000)
[7] F. Tedoldi, R. Santachiara and M. Horvatic, Phys. Rev. Lett. **83**, 412 (1999); J. Das, A. Mahajan, J. Bobroff, H. Alloul, Phys. Rev. B **69**, 144404 (2004)
[8] M. Takigawa, N. Motoyama, H. Eisaki, and S. Uchida, Phys. Rev. B **55**, 14129 (1997); N. Fujiwara, H. Yasuoka, Y. Fujishiro, M. Azuma, and M. Takano, Phys. Rev. Lett. **80**, 604 (1998)
[9] J. Bobroff, W.A. MacFarlane, H. Alloul, P. Mendels, N. Blanchard, G. Collin and J.-F. Marucco, Phys. Rev. Lett. **83**, 4381 (1999)
[10] F. Mila and T.M. Rice, Physica C **157**, 561 (1989)
[11] We used for the hyperfine couplings the values : $^{17}A_{hf}^c = 35.5kOe$, $^{89}A_{hf}^c = 2.0kOe$, $^{63}A_{hf}^c = -88kOe$ and $B = 22kOe$ which are determined with a typical accuracy of 10% [3]. This standard deviation mainly affects the value of the hyperfine field of ^7Li in the forthcoming analysis.
[12] Y. Itoh, T. Machi, C. Kasai, S. Adachi, N. Watanabe, N. Koshizuka and M. Murakami, Phys. Rev. B **67**, 64516 (2003)
[13] P. Mendels, J. Bobroff, G. Collin, H. Alloul, M. Gabay, J.-F. Marucco, N. Blanchard and B. Grenier, Europhys. Lett. **46**, 678 (1999)
[14] J.B. Boyce and C.P. Slichter, Phys. Rev. Lett. **32**, 61 (1974)
[15] Y. Sidis, P. Bourges, B. Hennion, L. P. Regnault, R. Villeneuve, G. Collin and J.-F. Marucco, Phys. Rev. B **53**, 6811 (1996)
[16] W. A. MacFarlane, J. Bobroff, H. Alloul, P. Mendels, N. Blanchard, G. Collin and J.-F. Marucco, Phys. Rev. Lett. **85**, 1108 (2000)
[17] We used here the data for τ given in ref [16] at 100K , and recalling that $h/\tau \propto ^7A_{hf}$, corrected by the ratio $1/2.5$ of the hyperfine fields determined here and estimated in ref [16]
[18] Y. Sidis, P. Bourges, B. Keimer, unpublished data (private communication)
[19] N. Bulut, Physica **363C**, 260 (2001); Y. Ohashi, J. Phys. Soc. Jpn. **70**, 2054 (2001)
[20] A.M. Finkel'stein, V.E. Kataev, E.F. Kukovitskii and G.B. Teitel'baum, Physica (Amsterdam) **168C**, 370 (1990); M. Gabay, Physica **235-240C**, 1337 (1994); D. Poilblanc, D.J. Scalapino, and W. Hanke, Phys. Rev. Lett. **72**, 884 (1994); N. Nagaosa and T.-K. Ng, Phys. Rev. B **51**, 15588 (1995); R. Kilian, S. Krivenko, G. Khal-iullin and P. Fulde, Phys. Rev. B **59**, 14432 (1999)
[21] J. Haase, D.K. Morr and C.P. Slichter, Phys. Rev. B **59**, 7191 (1999)
[22] A.J. Millis and H. Monien, Phys. Rev. B **54**, 16172 (1996); A. Goto, W. G. Clark, P. Vonlanthen, K.B. Tanaka, T. Shimizu, K. Hashi, P. V. P. S. S. Sastry and J. Schwartz, Phys. Rev. Lett. **89**, 127002 (2002)
[23] G. Aeppli, T.E. Mason, S.M. Hayden, H.A. Mook and J. Kulda, Science **278**, 1432 (1997)
[24] R.S. Markiewicz, cond-mat/0312595

- [25] H.A. Mook, P. Dai, S.M. Hayden, G. Aeppli, T.G. Perring and F. Dogan, *Nature* **395**, 580 (1998)



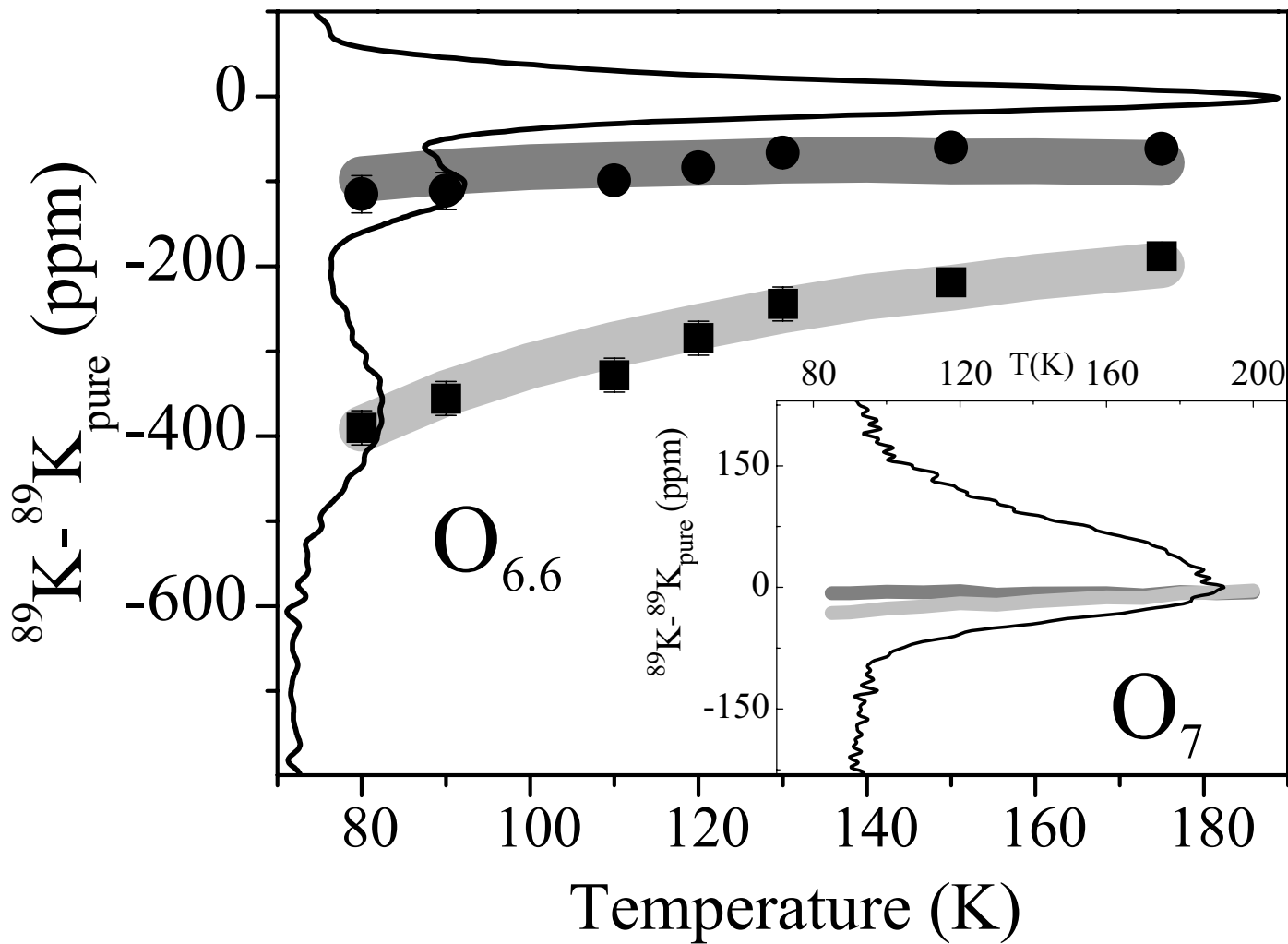


Figure 2
Ouazi *et al.*

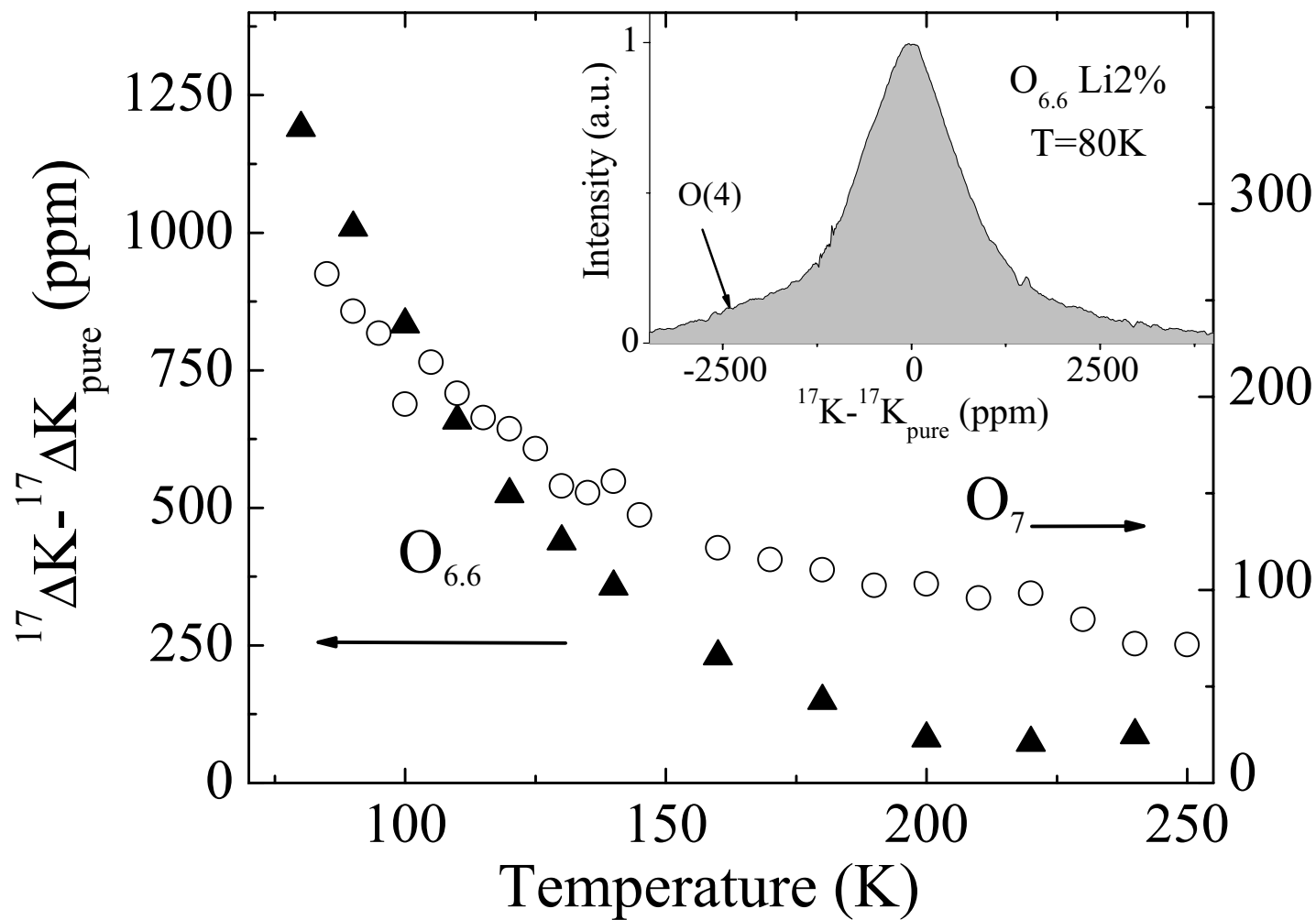


Figure 3
 Ouazi *et al.*

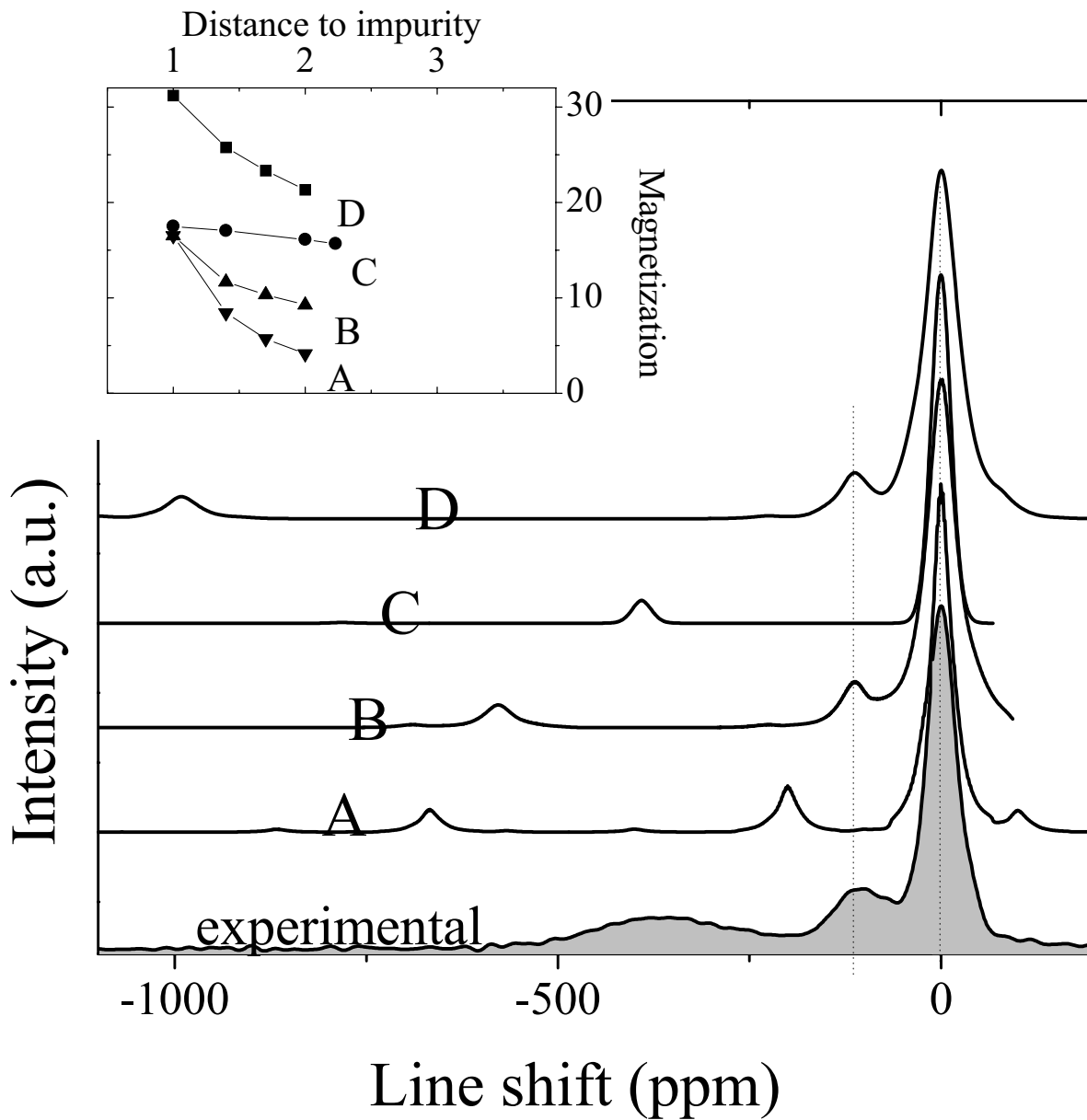


Figure 4
Ouazi *et al.*

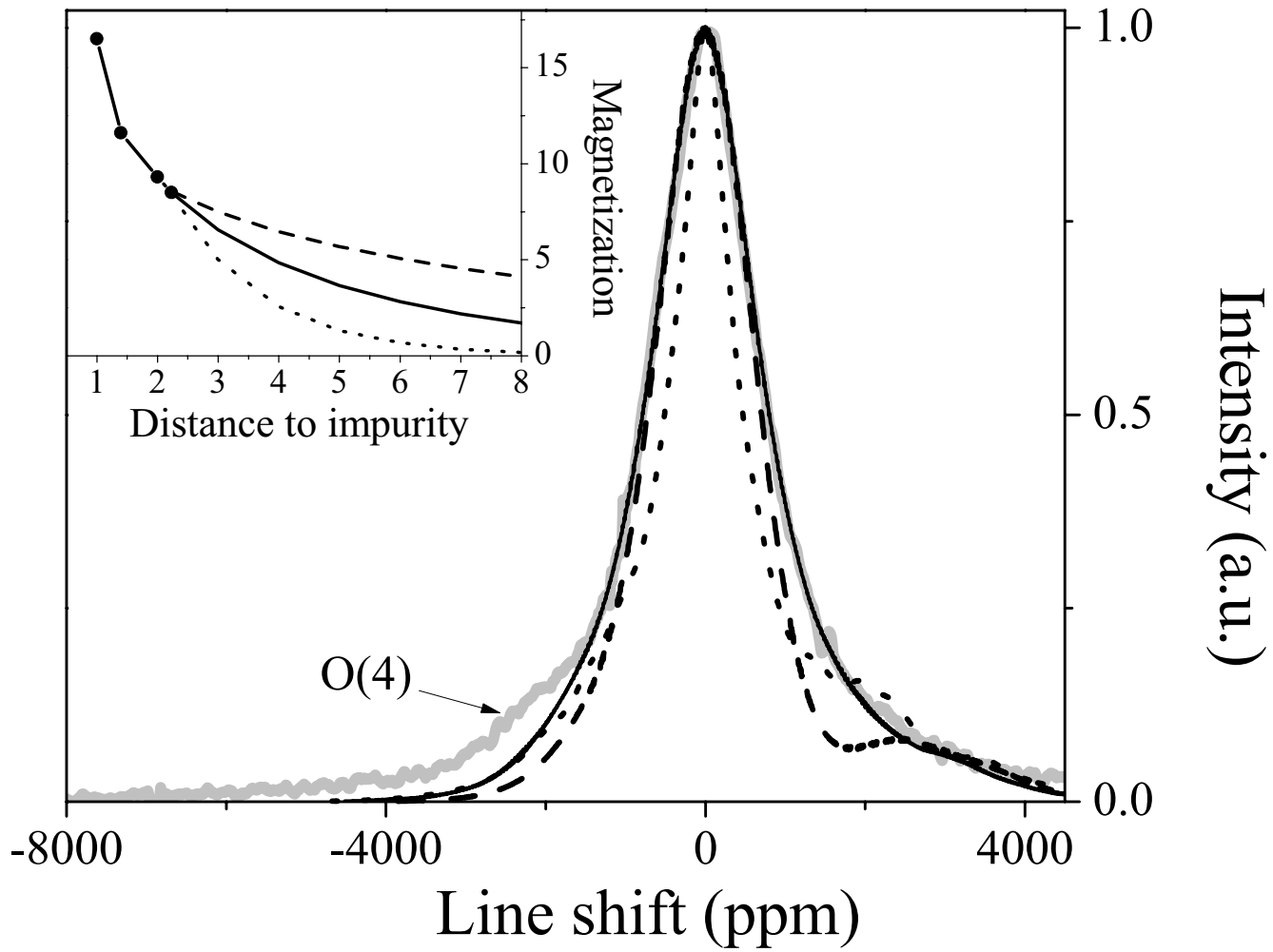


Figure 5
Ouazi *et al.*

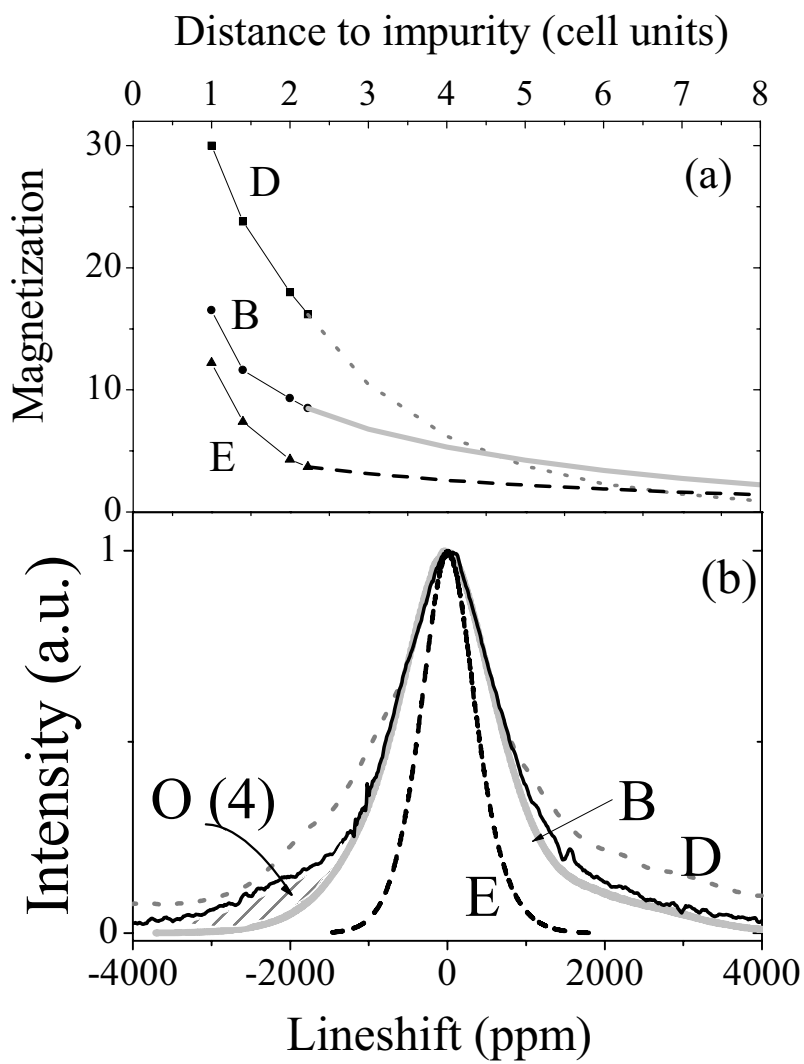


Figure 6
Ouazi *et al.*

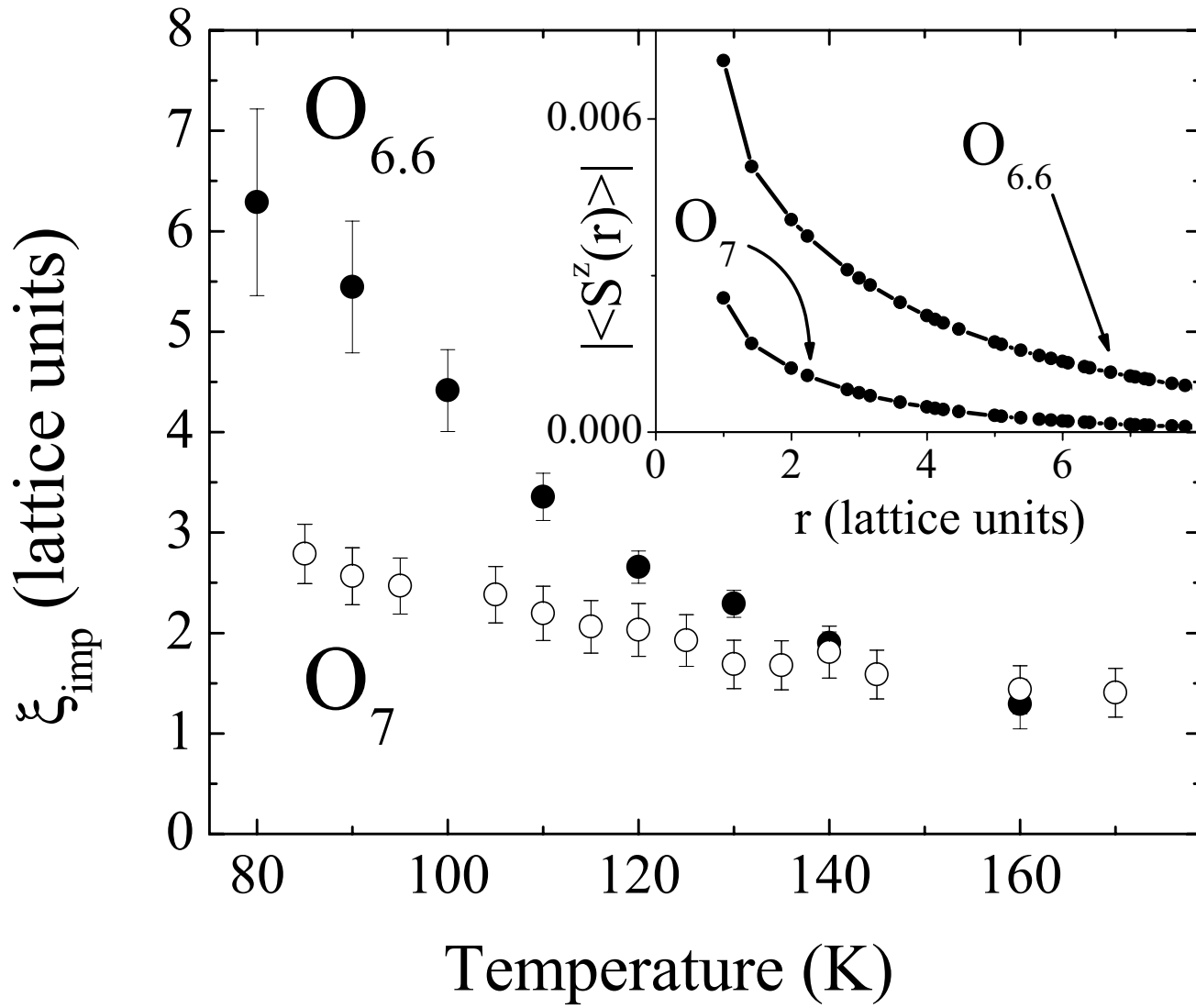


Figure 7
 Ouazi *et al.*

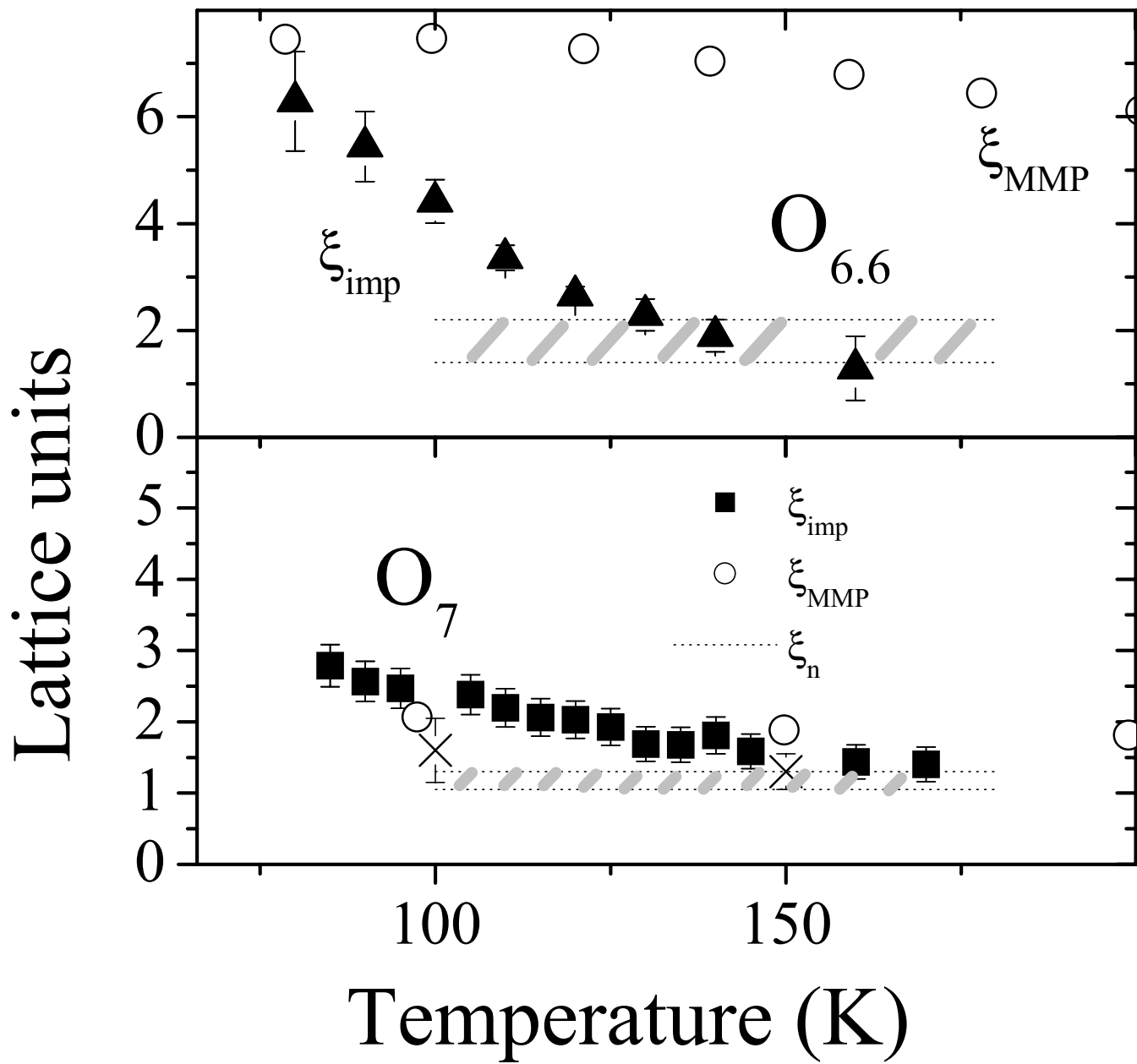


Figure 8
 Ouazi *et al.*